# Spreading of Lipid Monolayers on Hydrophilic Substrates at Increased Relative Humidities

Tobias Baumgart and Andreas Offenhäusser*

*Max-Planck Institute for Polymer Research, Ackermannweg 10, D-55128 Mainz, Germany*

*Received January 22, 2002. In Final Form: April 25, 2002*

A self-repairing ability of phospholipid monolayers deposited onto thin hydrogel films was observed by fluorescence microscopy, in terms of the expansion and lateral spreading of the monolayer into film defects. The spreading was quantitatively analyzed by covering half of a substrate supporting a thin hydrogel film with a lipid monolayer by Langmuir−Blodgett transfer and observing the spreading of the initially confined monolayer at increased relative humidities due to the hydration of both lipid headgroups and the polymer support. During the observation time of a typical spreading experiment, a constant spreading velocity was observed. A strong influence of monolayer pressure on the spreading velocity was observed. A nonlinear relationship between spreading velocity and monolayer pressure was found, which can possibly be explained by a dependence of the disjoining pressure in the monolayer/substrate interface on the monolayer pressure. The spreading velocity was additionally influenced by the kind of support and by the nature (e.g., phase state) of the deposited monolayer.

## Introduction

The phospholipid monolayer represents half of the bilayer, which is regarded to constitute, among other components, the compartmentalizing part of biological membranes.[1]

While the physicochemical parameters of phospholipid monolayers (more generally, Langmuir monolayers) at the air/water interface have been systematically and intensively studied for several decades[2] and are currently relatively well understood,[3] studies of substrate-supported phospholipid monolayers (more generally, Langmuir−Blodgett (LB) films) are relatively scarce[4] so far. However, recently interest has particularly grown, partially due to upcoming technical applications[5] and partially due to the invention of new approaches, especially the scanning probe techniques[6] such as STM (scanning tunneling microscopy),[7] AFM (atomic force microscopy),[8] NSOM (near-field scanning optical microscopy),[9] and related methodologies. Interest has especially been paid to the microscopic structure of supported phospholipid films. Both the film morphology directly after LB transfer and lateral reorganizations upon storage have been examined.[8,10] For the latter to take place, it has been observed that an increased relative humidity (RH) or the presence of other solvents in the gas phase is favorable.[10−13]

However, "surprisingly few studies have been made on the effects of humidity or other vapors on monolayer-coated surfaces exposed to ambient conditions".[11] Moreover, even the few works available in most cases only qualitatively describe the effects of changing the ambient humidity; quantitative assessments of the effect of RH on dynamic parameters of supported phospholipid monolayers are rare.[14]

Generally, biosensor applications based on model membrane systems demand a highly insulating membrane.[15] The substrate-supported lipid monolayer represents an intermediate stage in the fabrication of functionalized model membrane systems and therefore needs to be properly understood. Additionally, the monolayer stage allows for physicochemical studies, which would be more complicated, if not impossible, in the case of a lipid bilayer.

The structure of an initially deposited monolayer significantly influences the characteristics of the second monolayer deposited onto the first,[16] and therefore determines the quality of the resulting bilayer. Several processes can lead to film defects. Monolayer quality might be reduced due to mechanical distortions during the transfer process. Furthermore, deposition by Langmuir−Blodgett transfer inevitably comprises a drying step. If a polymer cushion is used as a membrane support,[17] during the drying step, thinning of the cushion might result in local, transient area changes, which could be inscribed into the lipid layer permanently due to reduced dynamics of lipid molecules in the dry state.

Obviously, an increased humidity will lead to a reduced motional coupling of the lipid layer to the hydrogel support,

---

* To whom correspondence should be addressed at the Institute for Thin Films & Interfaces (ISG2), Forschungszentrum Jülich, D-52425 Jülich, Germany. Phone: +49-2461-2330. Fax: +49-2461-61-2333. E-mail: a.offenhaeusser@fz-juelich.de.

(1) Singer, S. J.; Nicholson, G. L. *Science* **1972,** *175,* 720−731.
(2) Möhwald, H. *Annu. Rev. Phys. Chem.* **1990,** *41,* 441−476.
(3) McConnell, H. *Annu. Rev. Phys. Chem.* **1991,** *42,* 171−195.
(4) Fischer, A.; Sackmann, E. *J. Phys. (Paris)* **1984,** *45,* 517−527.
(5) Swalen, J. D.; Allara, D. L.; Andrade, J. D.; Chandross, E. A.; Garoff, S.; Israelachvili, J.; McCarthy, T. J.; Murray, R.; Pease, R. F.; Rabolt, J. F.; Wynne, K. J.; Yu, H. *Langmuir* **1987,** *3,* 932−950.
(6) Ivanov, G. R.; Petkova, J. I.; Okabe, Y.; Aoki, D.; Takano, H.; Kawate, H.; Fujihira, M. *Supramol. Sci.* **1997,** *4,* 549−557.
(7) Smith, D. P. E.; Bryant, A.; Quate, C. F.; Rabe, J. P.; Gerber, Ch.; Swallen, J. D. *Proc. Natl. Acad. Sci. U.S.A.* **1987,** *84,* 969.
(8) Chi, L. F.; Anders, M.; Fuchs, H.; Johnston, R. R.; Ringsdorf, H. *Science* **1993,** *259,* 213−216.
(9) Hwang, J.; Tamm, L. K.; Böhm, C.; Ramalingam, T. S.; Betzig, E.; Edidin, M. *Science* **1995,** *270,* 610−614.
(10) Shiku, H.; Dunn, R. C. *J. Phys. Chem. B* **1998,** *102,* 3791−3797.

(11) Chen, Y. L. E.; Gee, M. L.; Holm, C. A.; Israelachvili, J. N.; McGuiggan, P. M. *J. Phys. Chem.* **1989,** *93,* 7057−7059.
(12) Chi, L. F.; Johnston, R. R.; Ringsdorf, H. *Langmuir* **1992,** *8,* 1360−1365.
(13) Berman, A. D.; Cameron, S. D.; Israelachvili, J. N. *J. Phys. Chem. B* **1997,** *101,* 5692−5697.
(14) Baumgart, T.; Offenhäusser, A. Submitted for publication.
(15) Stelzle, M.; Weissmüller, G.; Sacmann, E. *J. Phys. Chem.* **1993,** *97,* 2974−2981.
(16) Merkel, R.; Sackmann, E.; Evans, E. *J. Phys. (Paris)* **1989,** *50,* 1535−1555.
(17) Sackmann, E. *Science* **1996,** *271,* 43−48.

which leads to enhanced diffusion and increased spreading velocity. Positive influences of the exposure of the monolayer to increased humidities are possibly the leveling out of local density gradients and the healing of voids or cracks in the monolayer film. The latter two types of defects have been observed by electron microscopy[4] and scanning probe microscopy techniques; see, e.g., ref 18. The healing of monolayer defects after the monolayer mobility is increased can be assumed to be due to either surface diffusion or a collective transport by spreading, or a combination of both transport mechanisms.[19]

The topic of the present work was to study the possibility of phospholipid monolayer spreading and the spreading characteristics upon exposure to a high ambient humidity. Monolayers were deposited onto thin, water-swellable polysaccharide films to reduce the frictional coupling between the monolayer and the underlying substrate. For comparison, monolayers were also transferred to and analyzed on glass supports. The influence of the substrate, the humidity, and the lateral pressure within the monolayer on the spreading behavior was analyzed.

The spreading of monomolecular amphiphile films on solids was analyzed in refs 20–23. Generally, a square root behavior of precursor film radius growth with a very sharp spreading front and a dense monolayer was found. Studies on the spreading behavior of trisiloxane oligo-(ethylene oxide) surfactants revealed that the ambient humidity influenced the spreading rates remarkably.

The spreading of phospholipid membranes on solid substrates thus far has been analyzed in terms of the spreading of bilayers deposited onto hydrophilic substrates.[24,25] The spreading of a single bilayer has been observed, with a spreading front displacement following a square root behavior with respect to the observation time.

The spreading of Langmuir–Blodgett monolayers (and of phospholipid monolayers in particular) on solid supports to the best of our knowledge so far has not been examined. This might partially be due to the fact that spreading on typical supports such as silicon oxide, glass, or mica is too slow. To circumvent this problem, in the present study, a water-swellable hydrogel was used for supporting the monolayer.

## Methods and Materials

**Fluorescence Microscopy.** Fluorescence microscopy was performed with an inverted microscope (IX 70, Olympus, Hamburg, Germany). A high-pressure mercury burner (HBO 100) served as light source. A fluorescence cube consisting of an excitation band-pass filter (BP 470-490, Olympus) and a barrier filter (BA 515, fluorescence cube U-MNIB, Olympus) was used. The lipid monolayer was observed through a transparent glass substrate (Mettler Glas, Rettberg, Göttingen, Germany; length 3.2 cm, width 2.6 cm, thickness 150–180 $\mu$m) by means of an oil immersion objective (100×, NA = 1.3; Zeiss, Göttingen). The substrate was mounted into a copper chamber (Figure 1), which allowed for the control of temperature and RH as described below. All spreading experiments were carried out at room temperature, i.e., 25 °C.
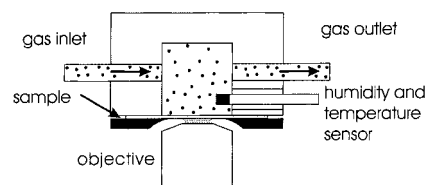


**Figure 1.** Humidity chamber for microscopic observation of supported lipid monolayers. The chamber walls were temperature-controlled by a water circle. The temperature and humidity sensor was thermally isolated from the chamber walls by a Teflon capsule. Prior to the objective being glued to the sample backside (microscopic coverglass), lipid on the backside of the coverglass was thoroughly wiped off with 2-propanol.

**Humidity Adjustment.** Spreading experiments were performed in a temperature- and humidity-controlled atmosphere. Lipid monolayers were enclosed in a copper chamber, which was sealed by the glass substrate (Figure 1). The RH inside the chamber was adjusted by the mixing of a dry and a water-saturated gas stream.[26] The dry gas was obtained by passing a nitrogen gas stream through a series connection of two silica-gel-filled bottles. The water-rich gas was produced by bubbling nitrogen through a series connection of two water-filled bottles. Computer-controlled valves (type 1259C-10000SV, MKS Instruments, Germany) allowed for changing the mixing ratio at a constant total flow. Care was taken to avoid water droplets from creeping along the gas tubes and entering the measurement chamber. Therefore, a water trap was inserted into the wet gas tube and the final part of the mixed gas tube was filled with cotton wool. The relative humidity was determined by measuring both the temperature and gas-phase water content in the chamber by a sensor, which was placed close to the substrate. The humidity and temperature sensor was a Hygroclip miniature air probe with an A1H interface, Rotronic, Germany. The transducer was equipped with an RS 232 interface, which enabled data readout by a PC. A feedback loop allowed for adjusting RH to the desired value.

**Langmuir–Blodgett Transfer.** The Langmuir–Blodgett method was used for preparing supported lipid monolayers. A trough with a mechanical dipper and Wilhelmy balance was used (NIMA Technology Ltd., Coventry, U.K.). The subphase consisted of ion-exchanged Millipore filtered water (Millipore Milli-Q system, $R$ = 18.2 MΩ cm). To cover only half of the substrate area with a lipid monolayer, the substrates were immersed halfway into the subphase[13] before transfer. Prior to spreading of the lipid solution, the polymer-covered substrates were equilibrated in the trough (for approximately 1/2 h) to allow for a smooth three-phase line to be established. Omitting the latter resulted in a final monolayer edge line with a pronounced roughness due to an inhomogeneous wetting of the polymer film (see Figure 4). Monolayers were obtained by spreading a lipid solution (chloroform, 1 mg/mL; all solvents used in the present work were p.a. quality) on the trough subphase. After the lipid solution was spread the solvent was allowed to evaporate (for a 1/4 h) and the film was compressed to the desired lateral pressure ($T$ = 25 °C). After completion of compression the film was deposited without further delay (at a speed of 4 mm/min) to avoid significant spreading of the monolayer onto the polymer support. To allow for visualization of the deposited monolayer by fluorescence microscopy, the lipid solution was doped by the addition of 1 mol % of a lipid fluorescence probe. Prior to mounting of the monolayer-covered glass substrates into the humidity chamber, lipid transferred to the backside of the substrate was thoroughly wiped off with a 2-propanol-soaked tissue.

**Lipids.** The lipids DMPC (1,2-dimyristoyl-*sn*-glycero-3-phosphatidylcholine), DSPC (1,2-distearoyl-*sn*-glycero-3-phosphatidylcholine), and cholesterol (3$\beta$-hydroxy-5-cholesten) were purchased from Avanti Polar Lipids, Alabaster, AL, and used without purification (the purity level was >99%, as stated by the manufacturer). The fluorescence probe used for staining the lipid monolayers was *N*-(7-nitrobenz-2-oxa-1,3-diazol-4-yl)-1,2-dihexadecanoyl-*sn*-glycero-3-phosphoethanolamine, triethyl-

(18) Sikes, H. D.; Woodward, J. T.; Schartz, D. K. *J. Phys. Chem.* **1996**, *100*, 9093–9097.

(19) Gaver, D. P.; Grotberg, J. B. *J. Fluid Mech.* **1990**, *213*, 127–148.

(20) Tiberg, F.; Cazabat, A.-M. *Langmuir* **1994**, *10*, 2301.

(21) Tiberg, F.; Cazabat, A.-M. *Europhys. Lett.* **1994**, *25*, 205–210.

(22) Villette, S.; Valignat, M. P.; Cazabat, A. M.; Jullien, L.; Tiberg, F. *Langmuir* **1996**, *12*, 825–830.

(23) Lucht, R.; Bahr, C. *Phys. Rev. Lett.* **2000**, *85*, 4080–4083.

(24) Rädler, J.; Strey, H.; Sackmann, E. *Langmuir* **1995**, *11*, 4539–4548.

(25) Nissen, J.; Gritsch, S.; Wiegand, G.; Rädler, J. O. *Eur. Biophys. J., B* **1999**, *10*, 335–344.

(26) Wolff, O. Ph.D. Thesis, Ruprecht-Karls-Universität, Heidelberg, Germany, 1998.

ammonium salt (NBD-PE; Molecular Probes, Leiden, The Netherlands). It was added to the lipid solution at a concentration of 1 mol % with respect to the host lipid.

**Polymer Cushions**. Chitosan and agarose were obtained from Fluka/Sigma Aldrich, Seelze, Germany, and used without purification. Chitosan was dissolved in a 1% v/v acetic acid solution (99.8%; Riedel-de Haën, Seelze)[27] at a concentration of 1% w/w with stirring overnight. The solutions were filtered through syringe filters (Millex, Millipore Corp., Bedford, MA) with a pore size of 5 $\mu$m. Afterward the solutions were centrifuged (Biofuge 22R, Heraeus, Germany) for 30 min at a speed of 11400 rpm. Thin chitosan films were prepared by spin-coating the chitosan solution onto cleaned, hydrophilic glass substrates. Substrate cleaning was performed by sonication in a 2% v/v Hellmanex solution (Hellma, Germany), followed by thoroughly rinsing the substrates in Millipore water. Spin-coating was typically performed at a spinning speed of 3000 rpm. Freshly prepared hydrogel layers were allowed to dry in air, for a period of typically 1/2 h. Ellipsometry measurements revealed film thicknesses around 140 nm. To neutralize the films, the polymer-covered substrates were immersed for several hours in a borate buffer (pH 9.22; Merck, Darmstadt, Germany) and afterward rinsed in Millipore water.

Agarose films were prepared by dipping clean substrates into a hot agarose solution of concentration 0.2% w/w. Upon quick withdrawal, a thin polymer film remained on the glass and formed a thin gel film during cooling.[28]

## Theoretical Background of the Dynamics of Spreading Processes

The spontaneous spreading of liquids on solid surfaces is controlled by the competition between driving terms and dissipative processes.[29]

The dynamics of a macroscopic droplet spreading on a solid can often be described by a relation known as the Tanner law.[30] From that law it follows that the velocity of the spreading droplet front is essentially independent of the spreading power $S$, which is the driving term for droplet spreading:

$$S = \gamma_S - \gamma_L - \gamma_{SL} \qquad (1)$$

with $\gamma_S$, $\gamma_L$, and $\gamma_{SL}$ being the interfacial tensions of the solid and liquid surfaces and the solid/liquid interface, respectively.

However, it has long been known that the spreading of a macroscopic liquid droplet on a solid is in many cases preceded by a very thin, invisible film,[31] which occurs even when condensation from a vapor phase can be neglected.[32] Whereas the shape of the macroscopic droplet is a thermodynamic, macroscopic property,[33] the surface profile of the precursor film is controlled by long-range surface forces (between approximately 30 Å and 1 $\mu$m[30]). Where evaporation can be neglected, the thickness of the "completely" spread droplet is above the value of a monolayer, even in the case of a zero (macroscopic) contact angle. Liquids with large $S$, however, spread more efficiently than liquids of small $S$. The independence of droplet spreading velocity on the spreading power can be explained by complete consumption of the free energy (per unit area), $S$, through dissipative processes in the precur-

sor film.[30] The spreading of films with mesoscopic thickness[29] can be described by continuum theories in terms of both statics (DLVO theory) and dynamics (hydrodynamics, Navier–Stokes equations).

Wetting of molecularly thin liquid films, however, is often accompanied by structuring effects. In fact, the films advance as a series of distinct molecular layers,[34] or—in later spreading stages—as a single monomolecular layer. While for macroscopic and mesoscopic films a no-slip boundary at the solid/liquid interface applies (the dissipation occurs in the bulk liquid, quantified by means of the viscosity $\eta$), in the case of molecularly thin layers dissipation occurs by friction at the solid support, on the molecular scale.

The monolayer growth of a simple liquid, extending from a straight reservoir or from a droplet of radius $R_0$, has been extensively studied experimentally, mainly by means of spatially resolved ellipsometry,[29,35-39] in combination with AFM,[40] or by spatially resolved surface plasmon spectroscopy.[23] Numerous theoretical investigations have been carried out.[41-45] In parallel, computer simulations[46] have been performed.

In most of the above-mentioned works monolayer spreading was found to follow a square-root behavior with respect to the time dependence of the spreading distance. In particular, the model developed in refs 43–45 leads to the following equation for a monolayer spreading from a bulk droplet with radius $R_0$:

$$R(t) = R_0 + A(D_0 t)^{1/2} \qquad (2)$$

In eq 2, $A$ is a parameter which may be positive (wetting), negative (dewetting), or zero and depends on temperature and particle/particle and particle/substrate interactions. $D_0$ is the diffusion coefficient of an isolated liquid molecule on the surface. Interestingly, $A$ depends mainly on liquid/liquid interactions and is almost independent of the spreading power.[44]

Apart from pure simple liquids, wetting of solids often occurs by or in the presence of surface-active compounds such as surfactants and lipid molecules. Wetting by amphiphiles is highly facilitated in the presence of water films ranging in thickness from the molecular to the macroscopic scale. The kinetics of spreading in these cases are accompanied by additional phenomena such as superspreading,[47] fingering instabilities,[48-50] and solitary waves.[51-53]

(27) Blair, H. S.; Huthrie, J.; Law, T.-K.; Turkington, P. *J. Appl. Polym. Sci.* **1987**, *33*, 641−656.

(28) Dietrich, C.; Tampe, R. *Biochim. Biophys. Acta* **1995**, *1238*, 183−191.

(29) Valignat, M. P.; Voue, M.; Oshanin, G.; Cazabt, A. M. *Colloids Surf., A: Physicochem. Eng. Aspects* **1999**, *154*, 25−31.

(30) de Gennes, P. G. *Rev. Mod. Phys.* **1985**, *57*, 827−863.

(31) Hardy, W. *Philos. Mag.* **1919**, *38*, 49.

(32) Bangham, D.; Saweris, S. *Trans. Faraday Soc.* **1938**, *33*, 554.

(33) Israelachvili, J. N. *Intermolecular and Surface Forces*, 2nd ed.; Academic Press: London, San Diego, New York, Boston, Sydney, Tokyo, Toronto, 1992.
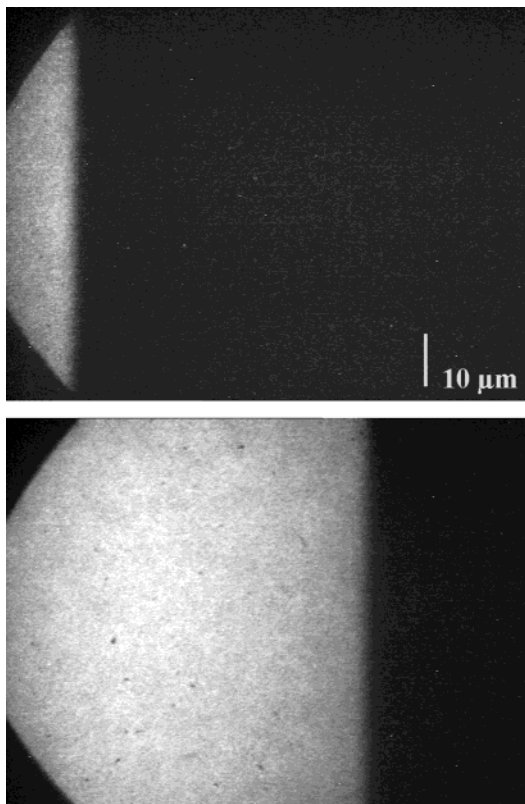
(34) Heslot, F.; Fraysse, N.; Cazabat, A. M. *Nature* **1989**, *338*, 640−642.

(35) Heslot, F.; Cazabat, A. M.; Levinson, P. *Phys. Rev. Lett.* **1988**, *62*, 1286−1289.

(36) Fraysse, N.; Valignat, M. P.; Cazabat, A. M.; Heslot, F.; Levinsson, P. *J. Colloid Interface Sci.* **1993**, *158*, 27−32.

(37) Cazabat, A. M.; De Coninck, J.; Hoorelbeke, S.; Valignat, M. P.; Villette, S. *Phys. Rev. E* **1994**, *49*, 4149−4153.

(38) Voue, M.; Valignat, M. P.; Oshanin, G.; Cazabat, A. M. *Langmuir* **1999**, *15*, 1522−1527.

(39) Blake, T. D.; Decamps, C.; De Conninck, J.; de Ruijter, M.; Voue, M. *Colloids Surf., A: Physicochem. Eng. Aspects* **1999**, *154*, 5−11.

(40) Villette, S.; Valignat, M. P.; Cazabat, A. M.; Schabert, F. A.; Kalachev, A. *Physica A* **1997**, *236*, 123−129.

(41) Abraham, D. B.; Collet, P.; Coninck, J. D.; Dunlop, F. *Phys. Rev. Lett.* **1990**, *65*, 195−198.

(42) Coninck, J. D.; Dunlop, F.; Menu, F. *Phys. Rev. E* **1993**, *47*, 1820−1823.

(43) Burlatsky, S. F.; Oshanin, G.; Cazabat, A.-M.; Moreau, M. *Phys. Rev. Lett.* **1996**, *76*, 86−89.

(44) Burlatsky, S. F.; Oshanin, G.; Cazabat, A.-M.; Moreau, M.; Reinhardt, W. P. *Phys. Rev. E* **1996**, *54*, 3832−3845.

(45) Oshanin, G.; De Coninck, J. D.; Cazabat, A. M.; Moreau, M. *J. Mol. Liq.* **1998**, *76*, 195−219.

(46) De Coninck, J.; Fraysse, N.; Valignat, M. P.; Cazabat, A. M. *Langmuir* **1993**, *9*, 1906−1909.

(47) Hill, R. M. *Curr. Opin. Colloid Interface Sci.* **1998**, *3*, 247−254.

**Figure 2.** DMPC monolayer on a chitosan film, lateral pressure 50 mN/m, relative humidity 90%: top, beginning of the spreading experiment; bottom, 9 min later. Note: the broadening of the spreading front during the spreading process was negligibly small.

The spreading dynamics of amphiphile monolayers on water films can be complex, and the form of the spreading law depends on the film thickness and monolayer geometry as well as on the ratio of the Marangoni driving term (surface tension gradient) to the diffusion coefficient; see eq 4. In the case of a constant film thickness, a constant spreading velocity proportional to the surface pressure gradient and the film thickness was found,[54] according to

$$\frac{\Delta\pi}{l} = \frac{\eta_w v}{d} \qquad (3)$$

where $\pi$ is the surface pressure, $l$ is the length of the spreading film, $\eta_w$ is the water viscosity, $v$ is the spreading velocity, and $d$ is the water film thickness.

### Results

The lateral expansion and spreading of lipid monolayers onto uncovered substrate areas was observed by fluorescence microscopy at increased relative humidities. At room humidity (RH $\approx$ 50%), however, the spreading velocity was too small to be detectable. Observation of the monolayer at room humidity right after the LB transfer revealed in most cases a sharp monolayer edge (Figure 2,

top). Only in cases where the lipid solution was deposited rapidly after the substrate was immersed into the LB trough a rough monolayer edge was observed (Figure 4), whereas equilibrating the substrate with the subphase prior to the deposition of lipid solution led to smooth monolayer edges. From the fluorescence intensity profile past the initial monolayer edge prior to performing a spreading experiment (Figure 3), it can be deduced that the edge width (about 1 $\mu$m) was in the range of the resolution of the optical microscope.

**Spreading of DMPC on Chitosan Surfaces**. Increasing the relative humidity to a value of RH = 90% substantially increased the monolayer mobility, which resulted in a movement of the spreading front (Figure 2, bottom). The kinetics of the spreading front displacement could be reversibly changed by altering RH, which indicates that spreading velocities were controlled by the water content of the surrounding gas phase, and not by the residual water content of the hydrogel layer stemming from immersion into the water subphase during the Langmuir–Blodgett transfer process. Accompanying the monolayer edge displacement, a slight broadening of the edge width occurred, as deduced from the intensity profiles shown in Figure 3. The intensity profiles were obtained by evaluating gray levels of pixels in a box-shaped region of interest and integrating along the direction of the monolayer edge line. The subtle broadening could be due to either a slight increase of the edge roughness or a small density gradient induced by spreading. Additionally, the reduced fluorescence intensity at the monolayer edge could be due to a higher friction of the fluorescence probe with the underlying support, compared to the unlabeled lipid molecules. Besides the slight intensity loss at the monolayer edge, the fluorescence intensity of the newly covered substrate area corresponded to the intensity observed in the initially covered area (see Figures 2 and 4).

As has been mentioned already, insufficient equilibration of the polymer cushion in the aqueous subphase led to a curvy monolayer edge. However, during the spreading process at an increased RH the edge structuring leveled out (Figure 4) while spreading over a distance of less than 100 $\mu$m. Also in Figure 4, it can clearly be seen that the intensity of the spreading monolayer is constant before and after spreading over a distance of dozens of micrometers.

Spreading experiments for time-dependent quantitative measurements were performed with samples where the spreading front appeared smooth right from the start. Monolayers were transferred at different lateral pressures, and the displacement of the spreading front relative to the starting position was determined at different spreading times. Figure 5 shows a typical development of the spreading front. In that experiment, a DMPC monolayer was transferred at a lateral pressure of 20 mN/m. The position of the monolayer edge was determined, and afterward, RH was set to 90%. An almost perfectly linear relation between spreading front displacement and time (Figure 5) was found for all lateral pressures, $\pi$, and RHs. The final spreading distance was in all cases below 90 $\mu$m, which is small compared to the initial total length (1.8 cm) of the monolayer. Hence, the monolayer expands only by a factor of <0.5% and therefore can be regarded as an infinite lipid reservoir.

Figure 6 shows the influence of the lateral film pressure (taken as the initial film pressure adjusted on the Langmuir–Blodgett trough during monolayer deposition) on spreading velocities of chitosan-supported monolayers at two different relative humidities (RH = 85% and 90%). The error bars were calculated from the error of linear fits

(48) Troian, S. M.; Wu, X. L.; Safran, S. A. *Phys. Rev. Lett.* **1989**, *62*, 1496–1499.

(49) Troian, S. M.; Herbolzheimer, E.; Safran, S. A. *Phys. Rev. Lett.* **1990**, *65*, 333–336.

(50) Elender, G.; Sackmann, E. *J. Phys. II* **1994**, *4*, 455–479.

(51) Borgas, M. S.; Grotberg, J. B. *J. Fluid Mech.* **1988**, *193*, 151–170.

(52) Jensen, O. E.; Grottberg, J. B. *J. Fluid Mech.* **1992**, *240*, 259–288.

(53) Frey, W.; Sackmann, E. *Langmuir* **1992**, *8*, 3150–3154.

(54) He, S.; Ketterson, J. B. *Philos. Mag. B* **1998**, *77*, 831–847.
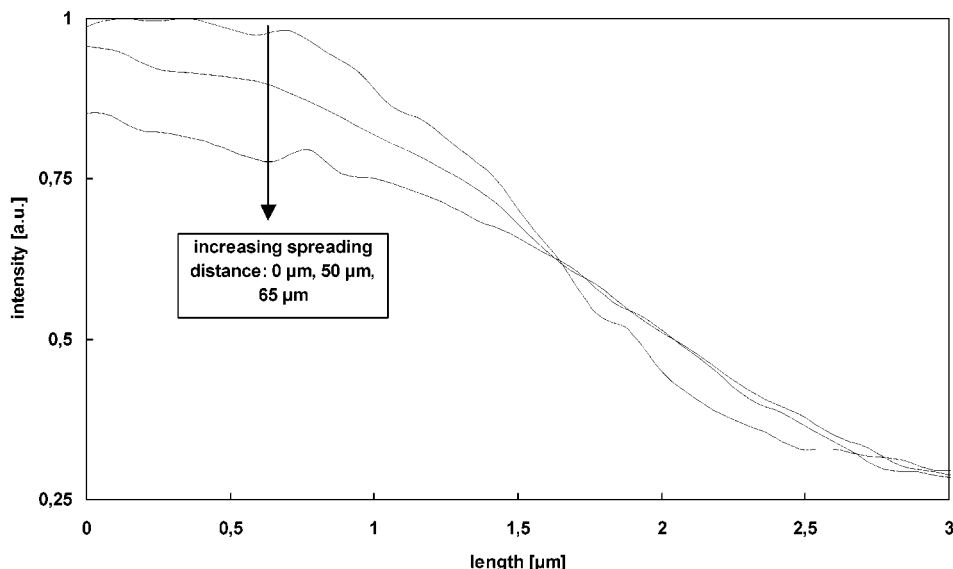
**Figure 3.** Intensity profiles of the monolayer edge (along a line orthogonal to the edge) during spreading. Note: the width of the edge prior to spreading is comparable to the resolution of the optical microscope. The intensity profiles have been shifted arbitrarily with respect to the length axis. Profiles were examined directly after deposition (0 $\mu$m), and after spreading over distances of 50 and 65 $\mu$m.
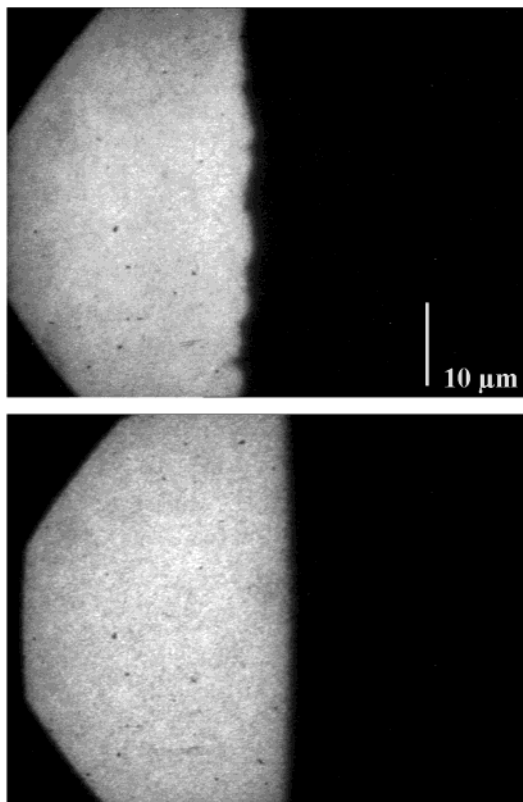


**Figure 4.** DMPC monolayer on a chitosan film, lateral pressure 20 mN/m, relative humidity 90%: top, prior to increasing humidity; bottom, 50 min later. In the case of the top picture, the sample had been shifted to compensate for the movement of the spreading front (approximately 40 $\mu$m).
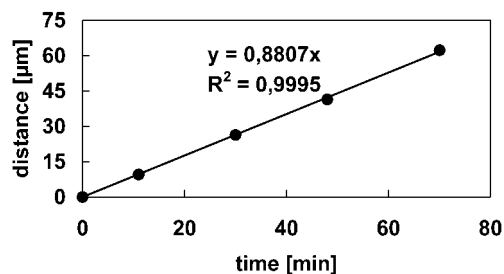


**Figure 5.** Spreading front displacement of a DMPC monolayer on chitosan, lateral pressure 20 mN/m, relative humidity 90%. The slope of a linear fit yielded a velocity of 0.88 $\mu$m/min, corresponding to 0.015 $\mu$m/s.
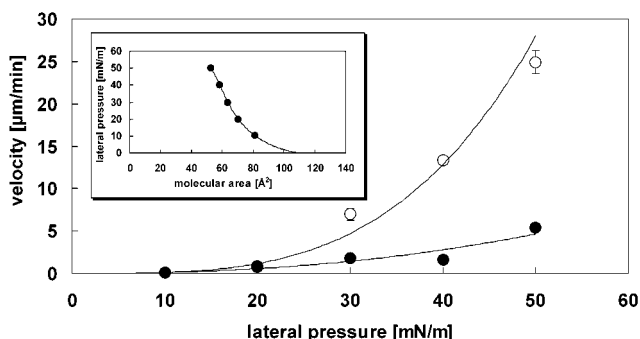


**Figure 6.** Comparison of the spreading velocities of DMPC monolayers transferred at different lateral pressures at two different relative humidities: closed circles: RH = 85%; open circles, RH = 90%. The lines are guides to the eyes. Inset: pressure/area isotherm of DMPC at 25 °C; the dots refer to the transfer pressures.

to the data series (Figure 5) and do not include error estimates from repeated measurements.

From the diagram, the following conclusions can be drawn: (I) RH showed a strong influence on the spreading velocity. In the case of a DMPC monolayer with a lateral pressure of 50 mN/m, a change of RH from 85% to 90% led to an increase of the spreading velocity from 5.3 to 25 $\mu$m/min, i.e., a factor of 4.7. (II) The lateral pressure set on the LB trough during monolayer deposition strongly influenced the spreading velocity. At a relative humidity of 90%, a change from $\pi = 10$ mN/m to $\pi = 50$ mN/m increased the spreading velocity from 0.1 to 25 $\mu$m/min, i.e., by a factor of 250. (III) The most interesting finding is that the relation between spreading velocity and lateral monolayer pressure $\pi$ was nonlinear, which is contrary to spreading of lipid on a water film of mesoscopic thickness.[54] Instead, the slope of an arbitrary fit to the data increases monotonically (Figure 5). At a lateral pressure of 50 mN/m at 25 °C, the DMPC monolayer was just in the coexistence
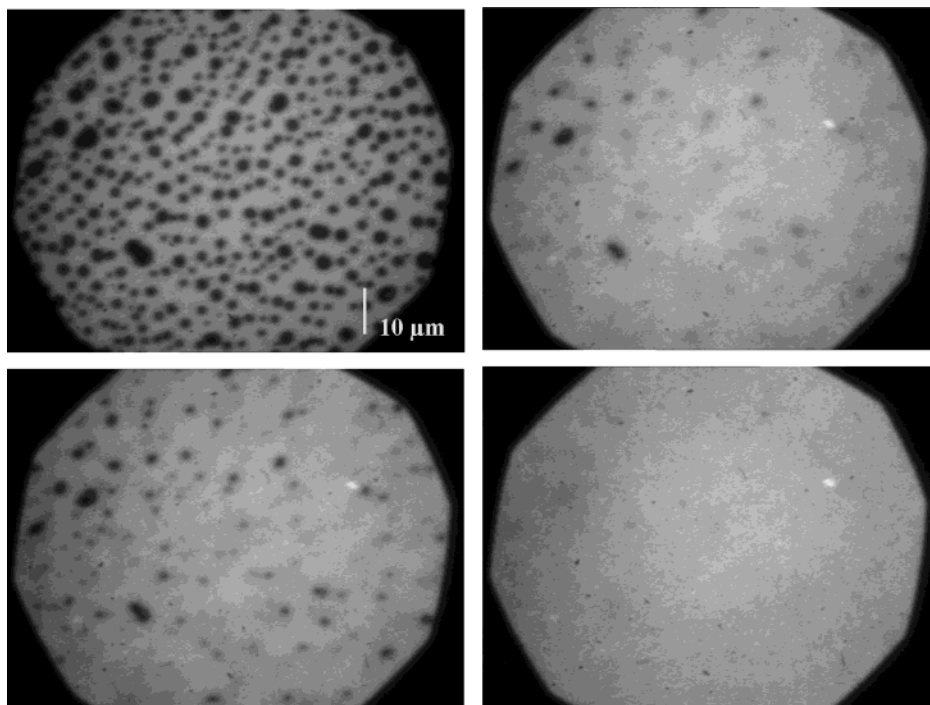
**Figure 7.** Fluorescence images showing (A, top left) the structure of a lipid monolayer (DMPC, lateral pressure 35 mN/m, fluorescence probe NBD-PC) which had been subjected to a condensation of water droplets, and which had been dried rapidly afterward, and (B, bottom left; C, top right; D, bottom right) the same location on the same monolayer as in (A), after switching to a high (near condensation) humidity. The time interval between each picture was approximately 1 min.

region, which, however, did not seem to influence the spreading velocity.

Figure 7 shows that monolayers resting on a hydrated polymer cushion at an increased relative humidity possess a self-healing property. Defects, which were caused by a condensation of water droplets on the monolayer surface due to a temperature gradient across the glass substrate, could be fixed in the monolayer by rapid dehydration. The condensation and evaporation of water droplets was followed by means of reflection interference contrast microscopy (RICM[24]). Interference patterns generated by this approach revealed a complete evaporation of water droplets during the dehydration step. Changing RH to a value just below the dew point caused a recovery of the initial homogeneous monolayer structure, i.e., a self-repairing by the lateral spreading of lipid into the monolayer holes.

**Spreading of DSPC and DMPC/Cholesterol Mixtures on Chitosan.** To analyze the influence of the phase state on the spreading behavior, a DSPC monolayer was transferred to a chitosan cushion at a lateral pressure of 40 mN/m, where DSPC is completely in the liquid condensed state. Figure 8 shows that, contrary to the case of a fluid monolayer (Figure 2), a relatively diffuse monolayer edge was obtained. Moreover, the film was rather inhomogeneous. It showed holes and cracks, which stem from the brittle condition of a condensed monolayer, in combination with a highly reduced mobility. In fact, raising RH even to values close to the dew point could not induce any observable spreading during the time of several hours.

Furthermore, the influence of the presence of cholesterol was examined. A DMPC monolayer with an additional amount of 30 mol % cholesterol was transferred onto a chitosan cushion at a lateral pressure of 40 mN/m at 25 °C. A spreading velocity of $0.16 \pm 0.009\ \mu$m/min was found at RH = 90%. Thus, the spreading velocity was reduced considerably compared to the value found for a pure DMPC
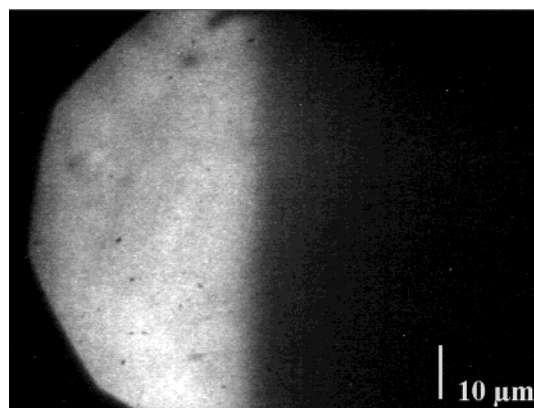


**Figure 8.** Monolayer edge of DSPC on chitosan, lateral transfer pressure 40 mN/m.

monolayer, transferred at the same conditions (spreading velocity at 40 mN/m and RH = 90%, $13.4 \pm 0.37\ \mu$m/min). The influence of cholesterol on supported membrane dynamics is manifold. Cholesterol reduces the diffusion coefficients measured in phospholipid membranes considerably.[55] Additionally, the presence of cholesterol leads to a dehydration of the membrane substrate gap,[25] which results in a further decrease in spreading velocity.

**Spreading of DMPC on Different Substrates: Agarose and Glass.** To demonstrate the influence of the nature of the monolayer substrate on spreading velocities, a DMPC monolayer with a lateral transfer pressure of 40 mN/m was deposited onto agarose and in a different experiment directly onto glass. In the case of the former, the spreading velocity at RH = 90% was $1.00 \pm 0.020$ $\mu$m/min, hence considerably smaller as compared to that of a DMPC monolayer on chitosan prepared and analyzed under the same conditions (see above). One reason for

(55) Almeida, P. F. F.; Vaz, W. L. C.; Thompson, T. E. *Biochemistry* **1992**, *31*, 6739−6741.

such a decrease of the spreading velocity is the pronounced roughness of agarose in comparison to chitosan. Additionally, it could be the case that the swelling behaviors of the polymer cushions chitosan and agarose are different.

On glass, the situation for a DMPC monolayer, lateral pressure of 40 mN/m at 25 °C and relative humidity of 90%, was similar to that of a DSPC monolayer on chitosan, exposed to the same conditions. On one hand, a clearly visible boundary between covered and uncovered substrate surfaces was observed (fluorescence picture not shown). On the other hand, no displacement of the spreading front was observed during several hours of exposure to extremely high relative humidities.

## Discussion

As indicated in Figures 2 and 4, a sharp boundary (at the resolution of the optical microscope) between monolayer-covered and uncovered substrates was obtained right after the LB transfer. In cases where insufficient equilibration of polymer-covered substrates in the LB trough caused a curvy three-phase line, the initially structured monolayer edge leveled out during spreading to yield an essentially straight line while spreading over a distance smaller than 100 $\mu$m. Furthermore, the monolayer edge width, which was below the resolution of the optical microscope before spreading, slightly increased during the spreading process. Moreover, the monolayer edge displacement velocity was strongly dependent on the lateral compression of the monolayer on the LB trough before transfer. These observations indicate that (I) spreading of the monolayer before the completion of the LB transfer, i.e., while the substrate was still immersed in the LB trough, can be neglected, (II) the position of the monolayer edge before spreading is determined by the position of the three-phase line in the LB trough before addition of lipid to the subphase surface, and (III) the lipid density at the monolayer edge is determined by the lateral pressure of the lipid monolayer on the LB trough.

The development of the meniscus at the three-phase line after addition of lipid solution to the subphase surface (*before* compression) was analyzed by Yaminsky et al.[56] These authors found that the three-phase line at a mica substrate, half immersed into a pure water subphase, retracts several hundreds of micrometers upon the addition of lipid solution (DSPE) onto the subphase. Upon retraction, the contact angle increased due to the deposition of lipid onto the solid, at a pressure of several mN/m, although the lateral pressure within the monolayer on the subphase was still below 0.1 mN/m. The contact angle (and therefore the lateral pressure of the monolayer deposited during meniscus retraction) depended on the amount of lipid solution initially loaded onto the subphase. The pressure difference between a monolayer deposited onto a substrate and that remaining on the LB trough subphase depends on the strength of the headgroup/substrate interaction.[56] As in the present work in most cases a hydrogel was used as a substrate, it can be assumed that the retraction of the initial three-phase line is grossly reduced, if not diminished completely. This assumption is supported by the observation that the spreading velocity did not depend on the amount of lipid solution added to the subphase surface, but on the lateral pressure obtained after compression of the monolayer on the LB trough.

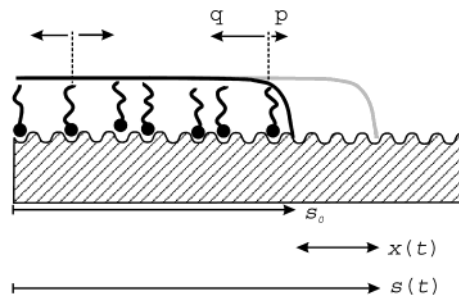The smooth spreading front of lipid monolayers is in contrast to the spreading front of phospholipid bilayers



**Figure 9.** Spreading of a lipid monolayer initially confined to a fraction of the whole substrate area. Molecules in the "bulk" film have the same transition probabilities in each direction. Boundary particles, however, have a higher tendency, $q > p$, to jump into the direction of the film, due to long-range attractive forces on the particle exerted by the monolayer. $s_0$ = initial length of the monolayer film, $s(t)$ = total length of the film at time $t$, and $x(t)$ = spreading distance at time $t$. The polymer supporting the lipid monolayer has been omitted for clarity.

on hydrophilic surfaces, where a steady roughening during spreading was observed.[14,24] The latter was explained by a percolation process: smooth spreading is obstructed by pinning centers at low spreading velocities. As the spreading coefficient in the case of monolayer spreading is much higher compared to that of bilayer spreading,[17] percolation due to pinning centers is likely to be reduced considerably.

Analyzing the dynamics of monolayer spreading revealed a linear relationship between the spreading front displacement and the observation time (Figure 5). The spreading velocity was dependent on monolayer pressure and the relative humidity.

The physical analysis of the spreading of a quasi two-dimensional layer on a solid can be reduced to a one-dimensional problem,[43] as depicted in Figure 9. In refs 43 and 57, particle dynamics were modeled as an activated random hopping transport constrained by hard-core (short-range) interactions between the local minima of potential wells in a square lattice (Figure 9). The wells are deep with respect to complete desorption to the gas phase, but act as a much lower barrier against the movement across the surface. Hops of diffusors only take place if the neighboring well is vacant. All particles, except those located at the film boundary, have isotropic transition rates: the probability to hop in any of the four directions is 1/4. However, at the film boundary transition rates are different: the probability, $q$, for a boundary particle to hop in the direction of the film exceeds the probability, $p$, to move toward the free surface. Advancement of the film, however, occurs because vacancies created by a boundary particle, while hopping toward the free surface, are filled by "bulk" monolayer particles. The asymmetry of transition rates at the boundary arises because of long-range (van der Waals) attractions. Thus, the "bulk" monolayer exerts a force on boundary particles, which drags them toward the film, and monolayer spreading can be regarded as liquid-like.

The hopping model proposed in refs 43 and 44 for monolayer spreading from an infinite bulk-liquid reservoir and applied to the spreading of a semi-infinite monolayer in a refined form in refs 45 and 57 predicts a square root behavior of the edge displacement with respect to the observation time.

According to ref 19, the ratio between advection-like spreading and spreading by diffusion is described by a

(56) Yaminsky, V.; Nylander, T.; Ninham, B. *Langmuir* **1997**, *13*, 1746−1757.

(57) Oshanin, G.; Coninck, J. D.; Cazabat, A. M.; Moreau, M. *Phys. Rev. E* **1998**, *58*, 20−23.

surface Peclet number, which in the present case reads

$$Pe = \frac{W_A}{\zeta D} \tag{4}$$

$W_A$ is the difference in surface energies of the covered and uncovered areas, $\zeta$ is a surface friction coefficient, and $D$ is the diffusion coefficient of an isolated molecule. Note that the definition of the Peclet number is lent from hydrodynamics, and for the quantity $\zeta$, the restrictions mentioned below hold. In the case of high Peclet numbers spreading by advection is favored. Spreading by advection leads to a constant spreading velocity as long as the pressure gradient $\Delta\pi$ across the spreading front is constant (see eq 3).

Borgas and Grotberg[51] theoretically predicted that the monolayer velocity on a thin water film is constant in the steady state (in the case of a constant monolayer length). In refs 50 and 54, a constant spreading velocity for monolayer spreading on a thin (mesoscopic) water film was found experimentally. He and Ketterson[54] studied the rate of lipid exchange between monolayers at different lateral pressures on two LB troughs, connected by a glass bridge covered by a thin water film. A linear dependence of monolayer velocity on the surface pressure difference, $\Delta\pi$, was found (eq 3) in the case of low velocities.

In the following, the time dependence of monolayer spreading will be analyzed by adapting a model which was proposed in ref 24 for the analysis of the spreading of a lipid bilayer on a solid substrate from an infinite reservoir. In ref 24, a stationary equilibrium is assumed; i.e., the gain in free energy per area, $W_A$, by bilayer spreading is equal to the energy dissipation by friction:

$$W_A \, dA = (f \, dy) \, ds \tag{5}$$

where $dA = dy \, ds$ is the area covered by the spreading film element ($y$ is the width of the proceeding rim) and $f$ is the viscous force per unit length of the proceeding rim. Further, a linear dependence of $f$ on sliding velocity, $v(s,t) = ds/dt$, as well as on the total length of the bilayer film is assumed:

$$f = \zeta \frac{ds(t)}{dt} s(t) \tag{6}$$

Combining eqs 5 and 6 then leads after integration to the spreading law

$$v(t) = \left(\frac{W_A}{2\zeta}\right)^{1/2} \frac{1}{t^{1/2}} \tag{7}$$

and hence to a $t^{-1/2}$ dependence of the spreading velocity. $\zeta$ is a viscous drag coefficient[24] which was interpreted in terms of a linear velocity gradient in the water film between the solid support and lipid membrane. Assuming no-slip boundaries at the membrane and solid surface yields $\zeta = \eta_w/d$, where $\eta_w$ is the bulk water viscosity and $d$ the thickness of the water film. Furthermore, dehydration of the membrane/substrate gap due to the presence of moderate amounts of cholesterol was found to lower bilayer spreading significantly.[25] In that case, $\zeta$ was interpreted as describing the friction between two monolayers, the first one (proximal layer) being fixed and the second one (distal layer) sliding over the first one. The meaning of $\zeta$ in the case of films with a thickness in the molecular range, however, is not obvious. In fact, what friction means at the molecular scale and which parameters are relevant is currently still a matter of debate.[29]

In the following, a model will be derived which follows closely the argumentation provided in ref 24. The main difference lies in the fact that, in ref 24, the spreading reservoir was a hydrated bilayer stack, whereas in the present case, the spreading reservoir is the monolayer itself. In the case of small spreading distances ($x(t) \ll s_0$; see Figure 9), the monolayer acts as an infinite reservoir. In the configuration depicted in Figure 9, the monolayer is initially confined to an area defined by length $s_0$ (and width $y$). Hence, the viscous force per unit length equation yields

$$f = \zeta \frac{ds(t)}{dt} s(t) = \zeta \frac{ds(t)}{dt} (s_0 + x(t)) \tag{8}$$

where the monolayer is assumed to behave rheologically as a Newtonian interface,[58] which is also assumed to be the case for direct friction with a solid support.[59] Additionally, it is supposed that dissipation occurs in a region with a length $s_0$, which is large compared to the spreading region $x(t)$. Whether $s_0$ refers to the whole initial monolayer length or to a region smaller than the whole monolayer, but much larger than the spreading front displacement $x(t)$ can in principle be proved by examining monolayer films with different initial lengths, which, however, was not carried out in the present work.

The parameter $\zeta$ in the present experimental configuration quantifies the viscous friction at the monolayer/substrate interface. Possibly, there might be an additional contribution of the dilational viscosity of the monolayer.[51,60,61] Combination of eqs 8 and 5 yields

$$(s_0 + x(t)) \, ds(t) = (s_0 + x(t)) \, dx(t) = \frac{W_A}{\zeta} \, dt \tag{9}$$

and after integration

$$s_0 x(t) + \frac{1}{2} x(t)^2 = \frac{W_A}{\zeta} t \tag{10}$$

With $s_0 \gg x(t)$, eq 10 reduces finally to

$$x(t) = \frac{W_A}{\zeta s_0} t \tag{11}$$

From eq 11 it follows that the spreading front displacement is proportional to the energy per unit area $W_A$ gained by spreading, and inversely proportional to the friction coefficient $\zeta$ and the length $s_0$ of the region in which dissipation occurs. Possibly, $s_0$ might correspond to a region with a smaller length than the initial film length. However, this does not affect the derivation of eq 11, as long as $s_0$ is much larger than $x(t)$. $W_A$ is the difference in surface energy of the monolayer-covered and the monolayer-free areas and may therefore be approximated by the monolayer film pressure $\pi$, which in the case of spreading of a monolayer onto a lipid-free area is equal to the difference in film pressures $\Delta\pi$. The spreading described by eq 11 therefore is driven by a Marangoni force, i.e., a surface tension gradient.

Thus, for small spreading distances, $x(t)$, in contrast to eq 7, a constant velocity is obtained, as long as $W_A/\zeta$ is constant. The latter condition is fulfilled if the monolayer

(58) Scriven, L. E. *Chem. Eng. Sci.* **1960**, *12*, 98−108.
(59) Evans, E.; Sackmann, E. *J. Fluid Mech.* **1988**, *194*, 553−561.
(60) Hirsa, A.; Korenowski, G. M.; Logory, L. M.; Judd, C. D. *Langmuir* **1997**, *13*, 3813−3822.
(61) Wüstneck, R.; Wüstneck, N.; Grigoriev, D. O.; Pison, U.; Miller, R. *Colloids Surf., B: Biointerfaces* **1999**, *15*, 275−288.

density reduction during spreading is small. The strong influence of the lateral pressure is in contrast to the diffusion model developed in ref 44, where a negligible influence of the spreading power (which is proportional to the lateral monolayer pressure; see eq 1) on the rate of monolayer growth was found. Thus, besides the constant velocity during spreading, the strong influence of the spreading power on the spreading velocity also favors the model developed above (eq 11).

The fluorescence intensity distribution over the whole spreading distance did not change significantly during spreading, which is contrary to the diffusion model developed in ref 43, where an s-shaped intensity profile was found in the spreading region, $x(t)$ (compare Figure 9). Therefore, besides the constant spreading velocity and the strong influence of monolayer pressure, the constant fluorescence intensity in the spreading region (apart from a slight increase of the monolayer edge width) also supports the assumption that monolayer spreading in the present case is dominated by advection.

According to Figure 6, the spreading velocity is strongly influenced by the relative humidity of the surrounding gas phase. For a given monolayer, $W_A$ should not depend remarkably on humidity; thus, the viscous drag coefficient $\zeta$ is the value responsible for changing spreading velocities with varying humidities. A linear relationship of spreading velocity and lateral monolayer pressure (for $W_A/\zeta s_0 =$ constant) was not found in the present experiments.

In all cases, monolayer dilation was below 0.5% of its original density. Hence, the influence of a shrinking monolayer reservoir can be neglected and therefore $W_A$ assumed to be constant. The observed nonlinearity can be explained by means of eq 11 by assuming that $\zeta$ depends on the lateral film pressure. One could argue that a change in headgroup density is accompanied by a change in the friction coefficient $\zeta$. In fact a hydrodynamic relation between $\zeta$ and the self-diffusion coefficient exists.[16,25,59] The self-diffusion coefficient, however, increases with decreasing monolayer density.[62] This effect would accelerate spreading at lower lateral pressures, which is not consistent with the data.

The influence of RH on $\zeta$ is possibly due to a change of the monolayer/substrate disjoining pressure, which in the present case is dominated by hydration forces.[33] It could be the case that the disjoining pressure depends not only on RH but also on $\pi$. In the case of protrusion forces causing the hydration force,[63] the prefactor of the exponential relation between disjoining pressure and separation distance depends on the protrusion site density. A reduced lateral pressure leads to a reduced protrusion site density, which could possibly result in a smaller hydration force, leading to increased friction in the case of monolayers with small lateral pressures.

In principle, the drag coefficient $\zeta$ can be determined by diffusion measurements and compared to those found from spreading experiments.[25] In the present case, however, the contribution of the dilational viscosity of the lipid monolayer to the dissipation is unknown. Furthermore, to be able to calculate $\zeta$ from spreading experiments, the length of the dissipation region must be known. Therefore, a comparison of friction coefficients obtained from spreading and diffusion experiments was not carried out.

The spreading velocity changed drastically while either the kind of monolayer support or the phase state of the deposited monolayer was varied. In the case of DSPC spreading on chitosan, according to eq 11, the friction coefficient $\zeta$ is highly increased. Thus, the magnitude of friction on the solid support is connected to the lateral fluidity of the monolayer membrane, which in the solid and in the fluid state can differ by several orders of magnitude.[62]

## Conclusion

A self-repairing ability of physisorbed amphiphile monolayers on hydrophilic substrates was observed and quantitatively analyzed by covering half of a planar hydrogel surface with a Langmuir–Blodgett film, raising the relative humidity considerably and examining the spreading kinetics of the monolayer onto the uncovered area. Directly after the transfer a very sharp and linear monolayer edge was observed, provided the hydrogel was equilibrated sufficiently with the trough subphase. In the case of film edge distortions being observed right after the transfer, these healed out quickly during the spreading process to yield a straight and sharp monolayer edge. This is in contrast to bilayer spreading, which was explained by the much higher spreading power in the case of monolayer spreading. A spreading front displacement linear with time was found for a lateral expansion of the monolayer of less than 0.5%. This was explained by assuming an expansion over a large film area and balancing the resulting dissipation by friction at the monolayer substrate interface with the driving force, the high surface energy of a free hydrogel surface. A simple model was derived which describes the dependence of the spreading velocity on the system parameters. The following features were found to influence the spreading dynamics: (I) the transfer pressure of the monolayer, (II) the relative humidity, (III) the phase state of the monolayer, (IV) the cholesterol content of the monolayer, (V) the nature of the substrate.

The dependence of the spreading velocity on the driving force was found to be nonlinear, in contrast to the spreading velocities obtained on a thin water film sublayer,[54] which could be explained by assuming that the friction at the monolayer/substrate interface varies with the monolayer density.

It is important to note that a retraction of the monolayer leading edge while the value of RH is *reduced* was never observed. In fact, in multibilayer stacks changing RH leads to an additional effective lateral pressure,[64] which compresses the bilayer and can therefore induce phase transitions (see, e.g., ref 65). In the case of a substrate-supported lipid monolayer, however, a lateral compression, which would be caused by a dehydration of the monolayer headgroups, would indeed be accompanied by a dewetting process. It is likely that (due to the much higher spreading power compared to a bilayer on a bilayer) dewetting is energetically so unfavorable that lateral-compression- and humidity-induced phase transitions in solid-supported monolayers are frustrated.

As already mentioned in the Introduction, the self-healing properties of Langmuir–Blodgett films might be of considerable importance for practical applications. The spreading power of bilayers on solid substrates is much lower compared to that of monolayers; therefore, the healing of monolayer defects *before* a second monolayer is deposited could be important for fabricating highly insulating bilayers.

(62) Peters, R.; Beck, K. *Proc. Natl. Acad. Sci. U.S.A.* **1983**, *80*, 7183–7187.

(63) Israelachvili, J. N.; Wennerstroem, H. *Langmuir* **1990**, *6*, 873–876.

(64) Parsegian, V. A.; Fuller, N.; Rand, R. P. *Proc. Natl. Acad. Sci. U.S.A.* **1979**, *76*, 2750–2754.

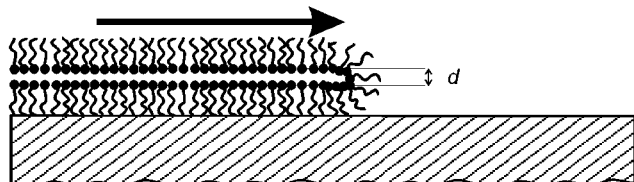(65) Binder, H.; Gutberlet, T.; Anikin, A.; Klose, G. *Biophys. J.* **1998**, *74*, 1908–1923.

**Figure 10.** Possible experimental configuration for correlating monolayer spreading with the water content of the lipid/lipid interface, i.e., the thickness of the water layer *d*. Spreading is due to the advancement of the upper monolayer, while the lower one is fixed on the substrate.

Many additionally important aspects of monolayer spreading could not be examined in the present work. Among these are a much more refined analysis of the quantitative influence of relative humidity on spreading velocity, the use of solvent gases different from water, and a deeper analysis of roughness effects on spreading velocities.

Due to the asymmetric monolayer/support interface, the effect of monolayer hydration could not be distinguished from the swelling of the polymer support. Additionally, the monolayer/substrate separation in a hydrogel-supported membrane is difficult to determine, due to the swelling of the polymer cushion over length scales much larger than the monolayer/substrate interface. These disadvantages could possibly be circumvented by spreading of a lipid monolayer on top of another monolayer, as depicted in Figure 10 for example. A hydrophobized substrate would be partially coated by Langmuir−Blodgett transfer. Subsequent withdrawal of the substrate would then result in an inverse bilayer (a solid-supported "foam film") with a defined bilayer edge. Substantially increasing RH should lead to a precisely measurable (e.g., by ellipsometry or surface plasmon resonance spectroscopy) change in the water layer thickness *d* (amounting to up to 3 nm[66]). Provided that the spreading front displacement is small compared to monolayer expansion, the spreading velocity should be determined by friction in the lipid/lipid interface lowered by repulsive hydration forces, and the spreading power. The water layer thickness in the case of monolayers with low lateral pressure, however, is determined not only by repulsive hydration forces but also by attractive hydrophobic forces as has been shown in the case of partially depleted bilayers by Helm et al.,[67] so additional phenomena can be studied.

(66) Rand, R. P.; Parsegian, V. A. *Biochim. Biophys. Acta* **1989**, *988*, 351−376.
(67) Helm, C. A.; Israelachvili, J. N.; McGuiggan, P. M. *Science* **1989**, *246*, 919−922.